Robotics and Computer–Integrated Manufacturing 51 (2018) 202–208

Contents lists available at ScienceDirect

Robotics and Computer–Integrated Manufacturing

journal homepage: www.elsevier.com/locate/rcim

Variable motion mapping to enhance stiffness discrimination and identification in robot hand teleoperation

Lingzhi Liu[a], Yuru Zhang[a], Guanyang Liu[a,*], Weiliang Xu[b]

[a] State Key Laboratory of Virtual Reality Technology and Systems, Robotics Institute, Beihang University, 37 Xueyuan Road, 100191 Beijing, China
[b] Department of Mechanical Engineering, The University of Auckland, Private Bag 92019, Auckland, New Zealand

ARTICLE INFO

Keywords:
Force feedback
Stiffness perception
Robot hand teleoperation

ABSTRACT

In robot hand teleoperation system, force feedback is critical for operator to perceive the physical property of grasped objects. However, it is challenging to implement accurate force feedback if the force accuracy of a haptic device is limited. This paper proposes a variable motion mapping method to enhance stiffness discrimination of the remote object. In this method, the motion mapping coefficient is regulated according to the object stiffness so that the operator can perceive the stiffness difference of the remote objects. To validate the proposed approach, we conducted two experiments on a three-finger robot hand (BarrettHand BH8-280) teleoperation system. In the first experiment, we measured the minimum relative change in feedback stiffness that could be detected by the operator. The result shows that the relative change should be 70% for a correct detection rate of about 91%. Based on the result, the motion mapping coefficient was selected for the system. In the second experiment, the variable motion mapping method was compared to a constant motion mapping method. The experimental task in the comparison is identifying four objects through stiffness perception alone. The experimental results show that the variable motion mapping method enhances the discrimination of the objects. The operator can identify individual object within a group of four without visual feedback with the variable motion mapping method.

1. Introduction

The purpose of using haptic feedback in teleoperation system is to enable operators to perceive the remote environment and enhance operational efficiency. To achieve this, the system must be transparent, i.e. the force perceived by the operator should be the actual force from the remote site. However, due to inertia, friction and backlash of the feedback devices, it is difficult to achieve perfect transparency [1]. In many applications, the transparency is redefined using task-specific performance criteria, for which the force feedback is required to benefit the operator to finish the task. For example, in teleoperated surgery, nonlinear and filtered force/position mappings were proposed to enhance stiffness discrimination of soft-tissue [2–4].

In this paper, we focus on teleoperation of robot hands in unstructured environment. Tele-control a robot hand to effectively grasp a wide variety of unknown objects is challenging. Since the objects have various properties, from soft to hard, light to heavy, fragile to solid. Visual feedback is essential for operators to acquire the position and shape of a grasped object for planning an effective grasp. Once a robot hand contacts the object, haptic feedback becomes dominant for the operator to perceive the interaction between the robot hand and the object [5]. Haptic feedback has been proved to enhance telegrasping performance [6–8]. High performance force sensors could be used in robot hand to measure the contact forces in remote environment accurately. Accordingly, haptic devices should also be able to provide accurate feedback force to operators. However, it is difficult for existing force feedback devices to accurately reproduce the force signals measured from slave side and render them to the operators.

Haptic gloves are the most commonly used master devices in robot hand teleoperation [9–13]. Lii et al. [11] used CyberGrasp as the master device to tele-control a robot hand in space. They found that the limitations in output force accuracy of CyberGrasp would restrict the grasp performance, especially with the grasping of deformable objects. Since the operator could not identify the object boundary based on force feedback, the telegrasping was much difficult. Peer et al. [12] used CyberGrasp to telemanipulate a BarrettHand. They mentioned that the quite huge friction in the tendons of CyberGrasp made it difficult to apply really small forces. Salvietti and Meli et al. [13,14] used two Omega.3 to telemanipulate a KUKA KR3 arm and the DLR-HIT Hand II. They proposed a method to map the motion of the master and slave devices having different structures. Monroy et al. [15] developed a multi-finger haptic interface for precise object grasping and collaborative manipulation. Liarokapis et al. [16] implemented a low cost force feedback device

* Corresponding.
E-mail address: gyliu@buaa.edu.cn (G. Liu).

https://doi.org/10.1016/j.rcim.2017.12.008
Received 10 November 2016; Received in revised form 29 December 2017; Accepted 29 December 2017

based on RGB LEDs and vibration motors to teleoperate a five fingered robot hand, DLR/HIT II.

This paper presents a method, called viable motion mapping, to enhance stiffness discrimination and identification of the grasped object in robot hand teleoperation. We aim to use low cost commercial haptic devices to achieve the goal. Stiffness relies on both force and displacement. Most impedance type haptic devices have limited force range, but their workspace is large enough for grasp motion mapping. We regulate the motion mapping coefficient between the master device and the slave robot hand based on real time estimation of the object stiffness. The feedback stiffness is adjusted with different coupling of motion and force feedback so that operators can perceive a clear difference in object stiffness.

A robot hand teleoperation system was constructed which includes a three-finger BarrettHand and a low-cost commercial haptic device, Falcon. Two experiments on this system were conducted. The purpose of the first experiment is to find out the minimum relative change of feedback stiffness that can be detected by the operator. Based on the result of this experiment, the change of the motion mapping coefficient can be determined to enhance the discrimination of the objects stiffness. To evaluate the performance of the proposed method, the second experiment was conducted in which the tasks was to identify remote objects through only haptic perception. The experimental results show that, compared to constant motion mapping method, the variable motion mapping method has better performance in the stiffness identification of the remote objects.

The following section introduces the principle of the proposed method. Section 3 describes the BarrettHand teleoperation system used as the test bed of the method. Section 4 describes the experiments and results for the system and Section 5 presents the conclusion and future work.

2. The variable motion mapping method

In this section, the principle of the variable motion mapping method for enhanced stiffness perception in robot hand teleoperation is presented. And the object stiffness estimation method is introduced.

2.1. Variable motion mapping

In teleoperation systems, motion mapping between the master side and the slave side can be defined as:

$$P_s = f(k_p, P_m) \tag{1}$$

where P_m and P_s represent the master and the slave motion (position or velocity) respectively, and k_p is the motion mapping coefficient with which the slave workspace is enlarged or reduced as compared to the master workspace. The value of k_p could be constant or variable depending on the system hardware capability and the task requirement. Similarly, the force mapping in teleoperation systems can be defined as:

$$F_s = f(k_f, F_m) \tag{2}$$

where F_m and F_s represent the master and the slave force respectively, and k_f is the force mapping coefficient.

The stiffness perception of teleoperation systems is based on the combination of the force (F) and the displacement (Δd) cues, which satisfies the stiffness definition $K = F / \Delta d$. Suppose the functions in formulas (1) and (2) are linear, the feedback stiffness in the master side K_m can be expressed as follows:

$$K_m = \frac{k_p}{k_f} K_s \tag{3}$$

where K_s is the object stiffness. The expression shows that the perceived stiffness in the master side is related to the motion and the force mapping coefficients in the teleoperation system.

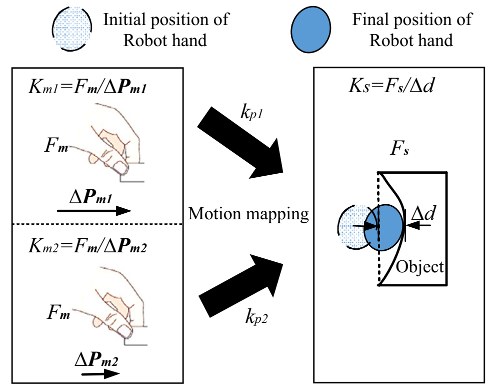

Fig. 1. The principle of variable motion mapping method for enhanced stiffness perception.

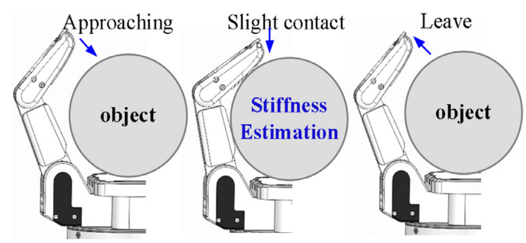

Fig. 2. Pre-contact step: object parameters estimation before real grasp.

In order to enhance stiffness perception in robot hand teleoperation, we propose a variable motion mapping method. The basic idea of the method is to change the feedback stiffness by regulating the motion mapping coefficient k_p. The force mapping is kept constant to guarantee the stability of the teleoperation system.

As illustrated in Fig. 1, an operator is tele-grasping an object with stiffness K_s. For the same slave displacement Δd, a smaller motion mapping coefficient ($k_{p1} < k_{p2}$) results in a larger master motion ($\Delta P_{m1} > \Delta P_{m2}$) which would make the operator feel that the object is softer as $F_m = F_s$. So by changing the motion mapping coefficient, an illusion of stiffness ($K_{m1} < K_{m2}$) can be achieved.

With the variable motion mapping, we can make soft objects feel even softer, and hard objects feel even harder. When setting a smaller value of k_p, the robot hand would move slower than the operator and the time achieving the same contact force would be longer. Thus, the perceived stiffness would be lower. In contrast, when setting a larger value of k_p, the robot hand would move faster than the operator and the time achieving the same contact force would be shorter, thus the perceived stiffness would be higher. In this way, we can use haptic devices with low output force resolution to distinguish different objects with similar stiffness.

2.2. Real-time stiffness estimation

In the variable motion mapping method, the motion mapping coefficient k_p is set based on real stiffness estimation of grasped objects. We consider teleoperation tasks in unknown environments. In such environments, the material and property of the objects are unknown. Therefore, a pre-contact step is defined to estimate the stiffness of an object in slave environment.

The first step of stiffness estimation is to make the robot hand contact the object with a restricted force and then leave it (see Fig.2). As in the following experiments, we set the maximum contact force to $2[N]$. Based on the contact force and finger motion information, the motion mapping coefficient can be estimated by using a stiffness computation model. Several models of stiffness computation [17–19] have been proposed in which the relationship between the penetration of the contacting bodies and the contact force were represented. We use Hunt-Crossley model [20] to estimate the contact impedance, which has been proved to be suitable for describing the contact dynamics of both stiff and soft objects. The model is formulated as:

$$F_i(t) = \begin{cases} k_i x_i{}^n(t) + \lambda_i x_i{}^n(t)\dot{x}_i(t), x_i \geq 0 \\ 0, x_i < 0 \end{cases} \tag{4}$$

where i = 1,2,3… represents the number of robot fingers. x_i is the penetration depth between the finger i and the object, which is calculated by the distance the finger moves after it initially contacts the object. F(t) is the contact force. k_i and λ_i are the elastic and viscous parameters which are determined by the stiffness and hardness of the grasped object. n is a constant number which relates to the geometry of contact surface. The online estimation algorithm in [19] is used to calculate the parameters k_i and λ_i with the following recursive equations:

$$\begin{cases} \theta(t+1) = \theta(t) + Q(t+1)[\varphi(t+1) - \mu^T(t+1)\theta(t)] \\ Q(t+1) = R(t)\mu(t+1)[\beta + \mu^T(t+1)R(t)\mu(t+1)]^{-1} \\ R(t) = [I - Q(t)\mu^T(t)]R(t-1)/\beta \end{cases} \tag{5}$$

where $\theta(t) = [k(t), \lambda(t)]^T \mu(t) = [x^n(t), x^n(t)\dot{x}(t)]^T \varphi(t) = F(t)$,$t$ represents the discrete time variable where the step size is 10 ms. β represents the forgetting factor limiting the estimation to more recent measure which is set to be 1 in this paper. $\theta(0) = [1, 1]^T$is chosen as the initial value for iteration.

We compute the elastic and viscous parameters from the estimation process for each finger based on the above mentioned algorithm. We assume that the material of the objects is homogeneous. The estimated stiffness K_s for the object is set by averaging the values k_i obtained for all the contact points:

$$K_s = \frac{1}{N}\sum_{i=1}^{N} k_i \tag{6}$$

where N represents the number of the contact points.

2.3. Determination of the motion mapping coefficient

According to Eq. (3), if the force mapping coefficient remain unchanged, the feedback stiffness difference ΔK_m is related to the estimated stiffness difference of objects ΔK_s and the motion mapping coefficient difference Δk_p:

$$\Delta K_m = \frac{K_s}{k_f}\Delta k_p + \frac{k_p}{k_f}\Delta K_s + \frac{\Delta k_p \cdot \Delta K_s}{k_f} \tag{7}$$

Combining Eqs. (7) and (3), we can derive the inequality:

$$\frac{\Delta K_m}{K_m} \geq \frac{\Delta k_p}{k_p} + \frac{\Delta K_s}{K_s} \tag{8}$$

The relative change of the feedback stiffness $\Delta K_m/K_m$ has a minimum value, K_{MRC}, under which the change in feedback stiffness can not be detected by the operator. The minimum value depends on the intrinsic limitation of the human perception and the technical limitations of haptic devices used in the teleoperation system. According to Eq. (8), if $\Delta K_s/K_s$ is larger than K_{MRC}, the object stiffness can be discriminated without changing the motion mapping coefficient k_p. Otherwise, if $\Delta K_s/K_s$ is smaller than K_{MRC}, k_p has to be changed to enlarge the feedback stiffness difference. In the variable motion mapping method, we change the motion mapping coefficient k_p based on the estimated stiffness K_s as follows:

$$k_p = \alpha K_s + C \tag{9}$$

where α is a scaling factor. C is a constant. The determination of the scaling factor α and the constant C should satisfies the following inequalities:

$$\frac{\Delta k_p}{k_p} > K_{MRC} = \min(\Delta K_m/K_m) \tag{10}$$

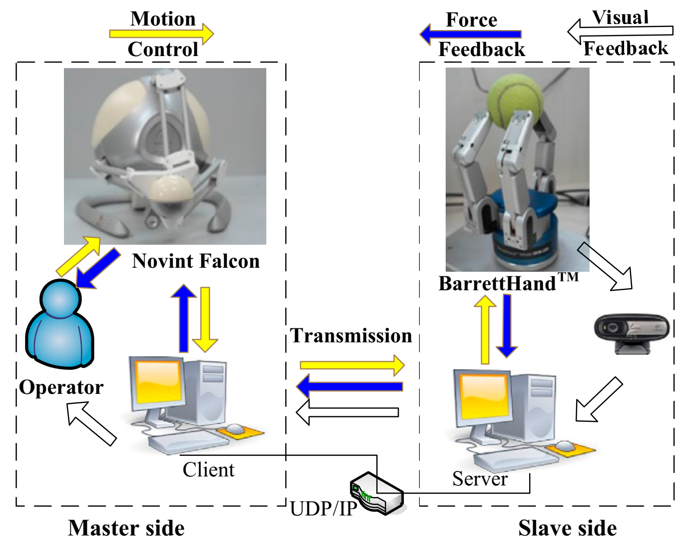

Fig. 3. The robot hand teleoperation hardware system.

In order to verify the effectiveness of the proposed method, a BarrettHand based teleoperation system was developed based on which two experiments were conducted as described in the following sections.

3. BarrettHand teleoperation system

This section introduces the BarrettHand based teleoperation system developed in our lab.

3.1. System structure

Fig. 3 shows the system structure. The robot hand on the slave side is a 4-DOF BarrettHand (BH8-280, Barrett Technology Inc.), which has three identical fingers (F1, F2, F3). The maximum output force at the tip of each finger is 2 kg. The motion range of the finger base joint is 140°. The BarrettHand has torque sensors installed at the distal joint of each finger. The range of each torque sensor is ±1 [Nm]. The accuracy of the torque sensors is 0.04 [Nm]. The values of strain gages in the torque sensors were calibrated relating the strain to the joint torque [21]. For most grasp tasks, the BarrettHand is flexible enough to generate a proper posture to grasp objects firmly.

A low-cost commercial desktop haptic device, Falcon (Novint Technologies Inc.), was used in the master side which provides a simple and intuitive interface for the operator [22]. The haptic device is a 3-DOF device with parallel kinematic structure. The handle of the device is a ball of 50 mm in diameter with four tool buttons on it. The maximum output force of the device is about 8.9[N]. The workspace of Falcon is 0.01m*0.01m*0.01 m. The parallel kinematic structure of the Falcon device looks quite similar to the grasp configuration of the robot hand with symmetrically distributed fingers as shown in Fig. 3. Therefore, it can provide an intuitive operating feeling for an operator. Meanwhile, it is relatively cheaper among those widely used haptic devices.

The BarrettHand and Falcon were connected by using a local network. The frequencies of haptic loop and network transmission are 1 KHz. A camera with USB interface was installed in the slave side and the real-time video was transmitted to the master side. The video and the simulated virtual robot hand were displayed in the master screen. A column bar showing the real-time contact force was displayed in the screen on which two marks showed the maximum pre-contact force and the maximum grasp force. The maximum pre-contact force is 2[N] and the maximum grasp force is 7[N] in our system.

Fig. 4 shows the control architecture of the robot hand teleoperation system. The object stiffness K_s is estimated in the model estimation and

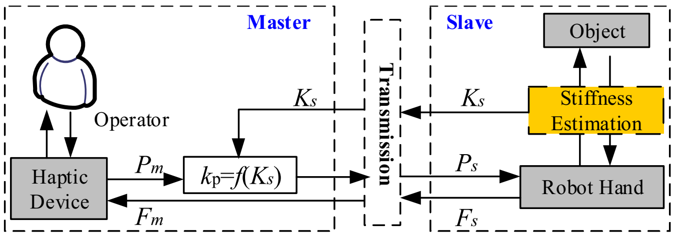

Fig. 4. System control architecture.

transmitted to the master side for calculating the motion mapping coefficient k_p. P_m and P_s represent the master and the slave motion respectively. F_m and F_s represent the master and the slave force respectively.

3.2. Robot hand motion mapping

The motion mapping in the system is designed based on the principle that the operator is able to complete operations as simple and intuitive as possible. The BarrettHand has two modes of motion: 1) fingers close and open, and 2) spread motion. In the first mode, the F1, F2, F3 fingers can close or open independently. In the spread motion, the F1 and F2 fingers can move around the hand palm synchronously.

We map the motion between the two sides in joint space to avoid solving inverse kinematic problem. Fig. 5 shows the motion mapping relationship. The Falcon device is 3-DOF parallel mechanism. When its end-effector moves in z-axis, the joint motions of each limb are similar to the bending and unbending of the robot finger. So the forward and backward motions along the z-axis of Falcon are mapped to the close and open motion of the fingers respectively. The spread motion of BarrettHand is controlled by the left and right motion (x-motion) of the Falcon ball hand.

The motion control of different fingers is switched by using the four buttons on the ball handle of Falcon. The operator can take control of each finger by pressing the corresponding button and release the control by pressing the button again. The F1, F2, F3 and spread buttons can be selected independently. The three fingers can move individually or together depending on which button is selected.

The position mapping between the haptic device and the robot hand is defined as:

$$\Delta\theta(t) = k_p \Delta P_{mz}(t) \tag{11}$$

where $\Delta\theta$(t) is the displacement of the finger joint. ΔP_{mz}(t) is the displacement of the haptic device alone the z axis. The default value of motion mapping coefficient k_p is 400°/m. This default value was selected to ensure that the joint velocities of the master device and the slave hand are basically the same.

3.3. Force feedback and contact detection

The grasping force on the fingertip F_{si} ($i = 1,2,3$) is calculated using the strain gage value S_{sgi}, assuming the contact point is at the fingertip. Because the maximum output force for Falcon (9[N]) is much smaller than the BarrettHand (20[N] for each finger), we scaled down the grasping force with the force scale factor k_f and set a maximum threshold as, $F_{si} < 15[N]$. The feedback force F_m in the master side is calculated as follows:

$$F_{\mathrm{m}} = k_f \left(\sum F_{si}\right)/3 \tag{12}$$

where k_f was set to be 0.7. The direction of the feedback force is in the z axis of the Falcon device. In this method, we assume that the grasps are always isotropic so that the forces are equally distributed at contact points.

During the grasping, one of the three fingers may reach the object firstly, which may result in an unexpected movement of the grasped object. To solve this problem, a coordination mechanism was designed in the system to guarantee all the fingers contact the object before they grasp the object. When a contact is detected between a finger and the object, the motion of the finger is suspended automatically until the other fingers contact the object. The grasp process started after all the fingers contact with the object. For each finger, we set a threshold of the strain gage value to detect the contact. The contact can be identified if the strain gage value is larger than the threshold. The threshold values were obtained from testing.

4. Experiment protocol

Two experiments were conducted on the BarrettHand teleoperation system. Fig. 6 shows the experimental setup. The BarrettHand and the master device were separately located in two rooms. Communication between the master and the slave sides was realized by a UDP/IP protocol and the time delay was negligible.

4.1. The minimum relative change of the feedback stiffness

The purpose of the first experiment is to find out the minimum relative change of the feedback stiffness K_{MRC} that can be detected by the operator in the BarrettHand teleoperation system. From Eq. (3), if the object stiffness K_s remain unchanged, the relative change of the feedback stiffness equals to that of the motion mapping coefficient:

$$\frac{\Delta K_m}{K_m} = \frac{\Delta k_p}{k_p} \tag{13}$$

So in the experiment, for a given object, different feedback stiffness is presented by changing the motion mapping coefficient. In the following, we measure the minimum relative change by a discrimination experiment.

4.1.1. Participants

Ten students, 7 male and 3 female, aged from 21 to 30, were paid to participate in the experiment. They were all right handed and familiar with the haptic device. All the participants had no experience in controlling a robot hand to grasp objects by using haptic device before. This study was approved by the Beihang university IRB and all participants signed an approved IRB consent form.

4.1.2. Procedure

Before the experiment, participants were instructed about how to use Falcon to control BarrettHand. And several sample objects were provided for the participants to get familiar with the grasping operation and the feedback during the operation.

The two-alternative forced-choice method was used in the experiment. In each trial, the participant was presented with a reference feedback stiffness, K_m (with the motion mapping coefficient k_p), and a test feedback, $K_m + \Delta K_m$ (with the motion mapping coefficient $k_p + \Delta k_p$). These two stimuli was presented randomly each time. After one trial, the participant was instructed to respond “1” or “2” to select which was stiffer between two stimuli. The reference motion mapping coefficient k_p were 400°/m. The test stimuli was decreased or increased with a constant step of 40°/m. And "1-up 1-down" rule was used in the experiment. After each incorrect response, the test feedback was increased. Conversely, after each correct response, the test stimuli was decreased. The experiment for one object ended if three continued reversals were obtained. The value of K_{MRC} was calculated using the average value of the three reversals. Two objects, an ocean ball and a water-filled bottle, were used in the experiment. We wanted to know if the value of K_{MRC} changes with different objects. Each participant did the experiment twice with the two objects respectively. Experiment session for one participant lasted about half hour, and they could take a break between runs whenever needed. The participant perceived the feedback stiffness through repeatedly grasping and releasing the object several times. The objects were held by the experimenter during the experiment.

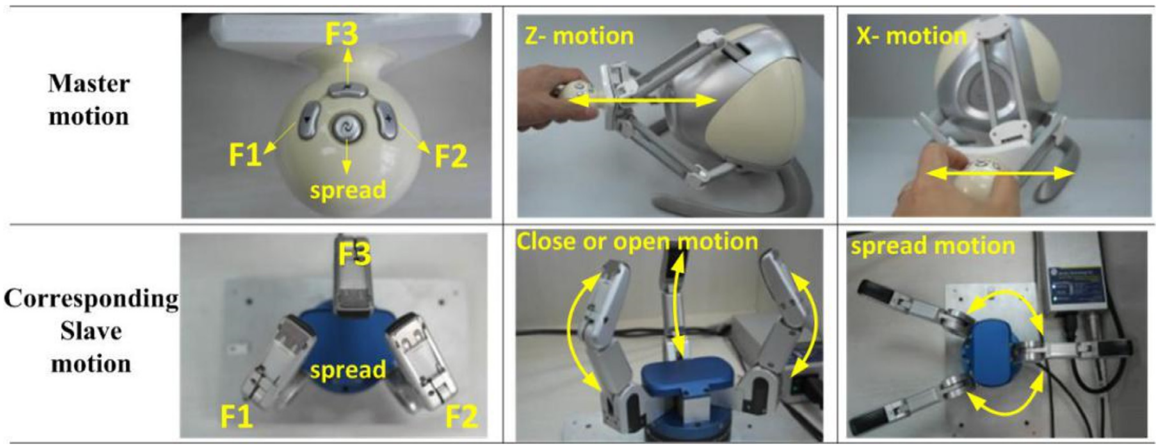

Fig. 5. Motion mapping between Falcon and BarrettHand.

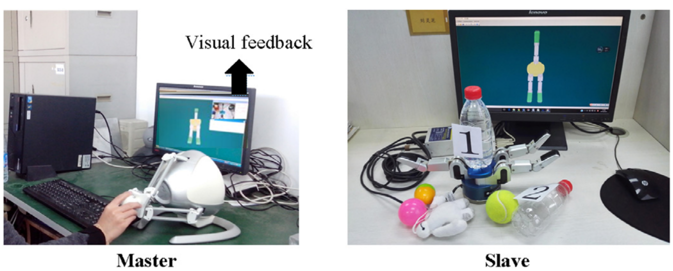

Fig. 6. Experimental scene.

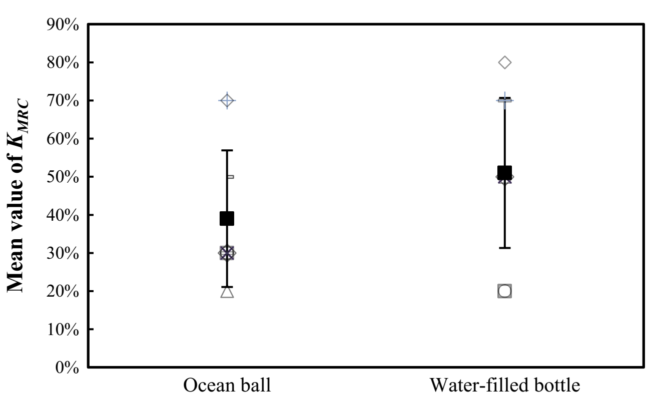

Fig. 7. The mean value of K_{MRC} for the two objects and the individual result of K_{MRC} for each participant.

4.1.3. Results

The experiment recorded two group of K_{MRC} values for the two experiment objects. Fig. 7 shows the result of the experiment. The paired *t*-test analysis in the SPSS statistical software shows that the difference between the mean values of K_{MRC} for the two objects is not significantly different ($t = -2.25$, $p > .05$). From the result, we can see that the difference in objects has no significant effect on the experiment result. The experiment counted the participants' trial number and the correct detection number for each test stimuli. We summed up the total number of the 10 participants and computed the corresponding correct detection rate which shows in the Fig. 8. From the figure, we can see that the relative change of feedback stiffness should be 70% ($\Delta k_p = 280$, $k_p = 400$) for a correct detection rate of about 91% for the BarrettHand teleoperation system.

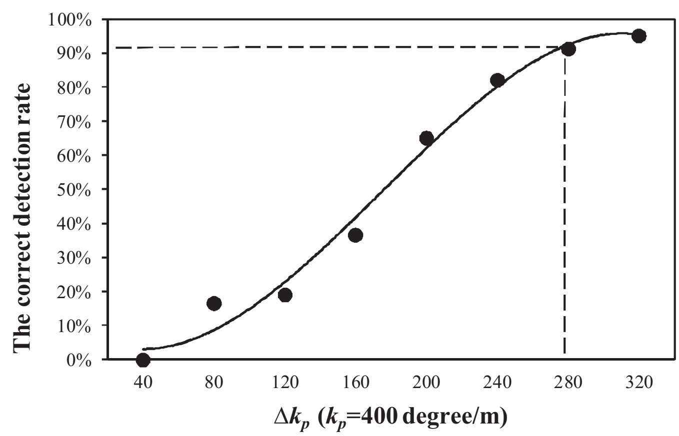

Fig. 8. The correct detection rate for each test feedback stiffness. The dashed line indicates the position of Δk_p is 280 and the corresponding correct detection rate is about 91%.

4.2. Object identification based on stiffness perception

In variable motion mapping method, we can adjust the motion mapping coefficient to enlarge stiffness difference between two objects based on the above experiment result, so that the stiffness discrimination is much easier. This would result in a problem that perceived stiffness is different from the real stiffness. How do we know the real stiffness of a remote object? In other words, how do we identify remote objects by perceiving their stiffness? In this experiment, we aim to verify that the operators can identify remote objects through stiffness perception after proper training. Again, we verify the effectiveness of the variable motion mapping method by comparing with the constant motion mapping method.

The experiment process consists of two phases: stiffness perception training and object identification. Participants were the same as in the first experiment.

4.2.1. Perception training

The training process was designed to train the participants to get familiar with the feeling of force feedback during object grasping so that they can identify the objects during the following tele-grasping. We choose a tennis ball and an ocean ball (see Fig.9) as the training objects. The stiffness difference between these two objects is so large that, even with the constant motion mapping, the participants can discriminate the two objects in teleoperation.

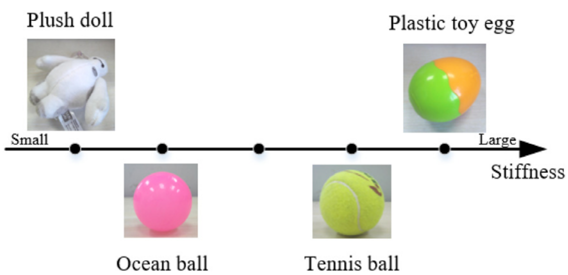

Fig. 9. The four objects used in the experiment.

During the training, participants were asked to grasp one of the two objects for five times and try to remember the stiffness perception of the object. The picture of training objects was displayed on the screen so that the participants knew which object they were grasping. Then the object was switched and the process repeated again. After the training, a test trial was conducted. The picture of the objects was removed and the participants were asked to distinguish the objects based on force feedback. If a participant fails, he/she should repeat the training process again until they succeeded.

4.2.2. Object identification

For object identification, we add two objects (plush doll, plastic toy egg) in the experiment. The purpose of the motion mapping is to enlarge the feedback stiffness difference among objects. In the experiment, the penetration depth x_i and the contact force F(t) in Eq. (4) were defined as the finger joint angle and the joint torque. We chose a median stiffness value according to the estimated stiffness of the four objects. The objects whose estimated stiffness is under 400 would be perceived softer, otherwise they would be perceived harder. So the mapping coefficient was calculated as follows:

$$k_{pi} = 1.5 \times (K_{si} - 400) + 400 \tag{14}$$

where i is the ID number of objects. All the four objects were arranged in the order of stiffness and displayed on the screen during the identification experiment as shown in Fig. 9. The relative differences of the feedback stiffness between each two objects in Fig. 9 are larger than 70% with the motion mapping coefficient determined by Eq. (14). The participants knew the stiffness difference among these objects shown on the screen. The experiment task is to identify the remote objects through stiffness perception. There were no visual feedback during tele-grasping. Participants identified the objects through comparing the perceived stiffness with that of the training objects. For example, if they feel the object is harder than the two training objects, they can tell that it is the plastic toy egg. For each object, the participants could try many times to grasp an object until they can identify it. After the trial for one object, the participants were asked to answer which object they thought the remote object was. There were 5 trials for each participant. Thus, one of the four objects would be selected twice. For each trial, the object was different and the order for each object to be grasped was randomly selected.

Each participant did the experiment twice with the variable motion mapping method and constant motion mapping method respectively. In the variable motion mapping method, the experiment process includes two steps: pre-contact and stiffness perception. In the pre-contact step, participants control the robot hand to slightly contact the object with the contact force less than 2 N for about 1 s and then release it. During the process, the object stiffness was estimated. After that the participant began to perceive the object stiffness through repeatedly grasping and releasing the object. In the constant motion mapping method, there is no pre-contact step, but only the stiffness perception. The default value of k_p in the constant motion mapping method is 400°/m.

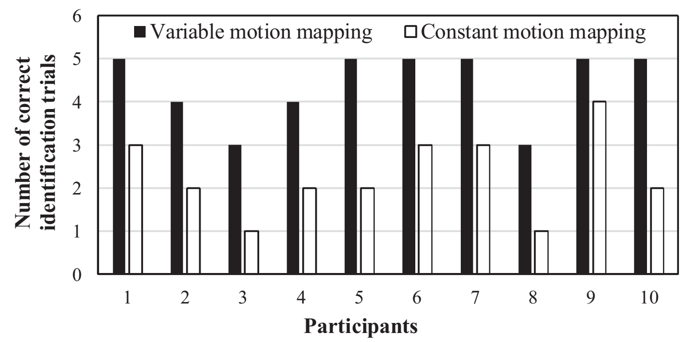

Fig. 10. The number of correct identification trials for each participants.

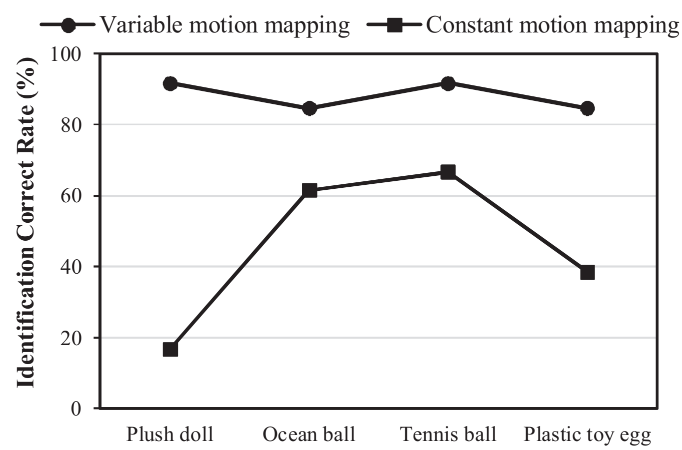

Fig. 11. The identification correct rate for the objects with the two motion mapping methods.

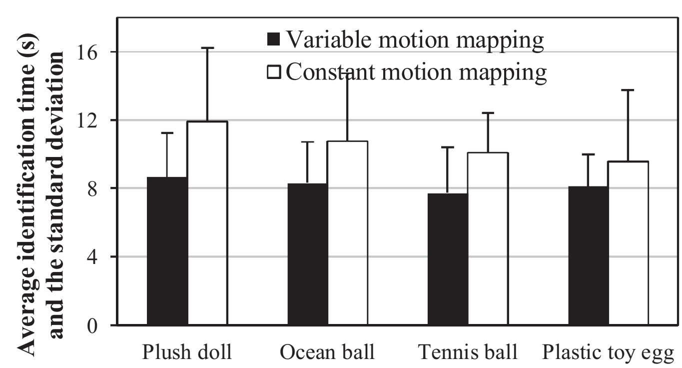

Fig. 12. The average identification time for the objects with two motion mapping methods.

4.2.3. Experimental results

Fig. 10 shows the number of correct identification trials for each participant with the variable motion mapping and the constant motion mapping. From the figure, we can see that six of the ten participants could correctly identify all the objects with the variable motion mapping. But with the constant motion mapping, none of the 10 participants could identify all the objects correctly. Fig. 11 gives the identification rate of each object. The results show that the correct identification rates were above 85% for the variable motion mapping,but below 70% for the constant motion mapping. In particular, the rates of plush doll (20%) and plastic toy egg were much lower than that of the two training objects. The stiffness differences between plush doll and ocean ball, and between tennis ball and plastic toy egg were so small that they were hard to be identified with the constant motion mapping.

Table 1
The ANOVA results of the average identification time.

Objects	Sample size (trials)	F	p-value(<.05)
Plush doll	12	4.927	.037
Ocean ball	13	3.614	.069
Tennis ball	12	5.403	.030
Plastic toy	13	1.377	.252

Fig. 12 shows the average time the participants used to identify each objects correctly. The ANOVA analysis for the average identification time was shown in Table 1. We found that the average identification time for the variable motion mapping is less as compared to the constant motion mapping. However, the difference of the identification time for plastic toy egg and ocean ball is not significant. The result indicated that the identification efficiency of plush doll and tennis ball was improved by using the variable motion mapping method. But not all the identification efficiency was improved. The efficiency evaluation for the proposed method needs for further study.

5. Conclusion

It is challenging for current haptic interfaces to provide force feedback for tele-grasping with desirable transparency. In order to overcome the limitation of current haptic interface for grasping operation, this paper proposed a variable motion mapping method for stiffness perception in robot hand teleoperation. The key idea of the proposed method is to regulate the motion mapping coefficient according to the object stiffness which is estimated in a pre-contact phase before object grasping.

The proposed method was verified on a BarrettHand teleoperation system. We found througth the first experiment that the relative change in feedback stiffness should be 70% for a correct detection rate of about 91%. Based on the result, the motion mapping coefficient was selected in the second experiment for the identification of object using stiffness perception. We show that with appropriate training, the variable motion mapping method allows operators to identify individual object within a group of four without visual feedback. The results also show that, with the variable motion mapping method, operators can identify more objects than with the constant motion mapping. Our study demonstrate that the variable motion mapping method can enhances the discrimination and identification of object stiffness in the robot hand teleoperation.

One limitation of our method is that the object stiffness needs to be estimated in real-time at slave side by pre-contact. This would decrease the efficiency of teleoperation. However, in the case that the remote objects are hard to be identified by stiffness, this method can be more efficient than the constant motion mapping.

Acknowledgments

This work was supported by China domestic research project for The project for International Thermonuclear Experimental Reactor (ITER) is funded by the National Science and Technology Major Project [grant numbers 2012GB102006, 2012GB102008] and the Open Research Fund of Key Laboratory of Space Utilization, Chinese Academy of Sciences (No. LSU-YKZX-2017-01).

References

[1] H Li, K Kawashima, Bilateral teleoperation with delayed force feedback using time domain passivity controller[J], Rob. Comput. Integr. Manuf. 37 (C) (2016) 188–196.
[2] P Malysz, S Sirouspour, Nonlinear and filtered force/position mappings in bilateral teleoperation with application to enhanced stiffness discrimination[J], IEEE Trans. Rob. 25 (5) (2009) 1134–1149.
[3] X Wang, X Liu P, D Wang, et al., Design of bilateral teleoperators for soft environments with adaptive environmental impedance estimation[C], in: *Robotics and Automation,* 2005. ICRA 2005. Proceedings of the 2005 IEEE International Conference on, IEEE, 2005, pp. 1127–1132.
[4] C Cavusoglu M, A Sherman, F Tendick, Design of bilateral teleoperation controllers for haptic exploration and telemanipulation of soft environments[J], Pap. Sci. Technol. 18 (4) (2013) 641–647.
[5] T Gibo, A Bastian, A Okamura, Grip force control during virtual object interaction: effect of force feedback, accuracy demands, and training, IEEE Trans. Haptic. (99) (2013) 1–1.
[6] M. Zafar, D.C.L.V. Doren, Effectiveness of supplemental grasp-force feedback in the presence of vision, Med. Biol. Eng. Comput. 38 (3) (2000) 267–274.
[7] E.P.W. Van der Putten, J.J. van den Dobbelsteen, R.H.M. Goossens, et al., The effect of augmented feedback on grasp force in laparoscopic grasp control[J], IEEE Trans. Haptic. 3 (4) (2010) 280–291.
[8] R.D. Howe, D. Kontarinis, Task performance with a dexterous teleoperated hand system, in: Proc. SPIE1833, Telemanipulator Technology, 1993 (March 26, 1993).
[9] Y. Yoshimura and R. Ozawa. A supervisory control system for a multi-fingered robotic hand using datagloves and a haptic device, *2012* IEEE/RSJ International Conference on Intelligent Robots and Systems, October 7–12, 2012. Vilamoura, Algarve, Portugal, pp.5414–5419.
[10] H. Shao, K. Nonami, T. Wojtara, et al., Neuro-fuzzy position control of demining tele-operation system based on RNN modeling[J]., Rob. Comput. Integr. Manuf. 22 (1) (2006) 25–32.
[11] N.Y. Lii, Z. Chen, B. Pleintinger, C.H. Borst, G. Hirzinger, A. Schiele, Toward understanding the effects of visual- and force-feedback on robotic hand grasping performance for space teleoperation, in: *The 2010 IEEE/RSJ International Conference on Intelligent Robots and Systems*, October 18–22, Taipei, Taiwan, 2010, pp. 3745–3752.
[12] A. Peer, S. Einenkel, M. Buss, Multi-fingered telemanipulation - mapping of a human hand to a three finger gripper, in: *The IEEE International Symposium on Robot and Human Interactive Communication*, 2008, Ro-Man, 2008, pp. 465–470.
[13] Gionata Salvietti, et al., Multicontact bilateral telemanipulation with kinematic asymmetries, IEEE/ASME Trans. Mechatron. 22 (1) (2017) 445–456.
[14] Leonardo Meli, et al., Multi-contact bilateral telemanipulation using wearable haptics. *Intelligent Robots and Systems (IROS)*, 2016 IEEE/RSJ International Conference on, IEEE, 2016.
[15] Mary Monroy, et al., Masterfinger: multi-finger haptic interface for collaborative environments, Haptics: Perception, Devices and Scenarios (2008) 411–419.
[16] M.V. Liarokapis, P.K. Artemiadis, K.J. Kyriakopoulos, Telemanipulation with the DLR/HIT II robot hand using a dataglove and a low cost force feedback device, Control Autom. (2013) 431–436.
[17] X. Mu, Q. Wu, On impact dynamics and contact events for biped robots via impact effect, *IEEE Trans. Syst. Man Cybern.* Part B 36 (6) (2006) 1364–1372.
[18] G. Gilardi, I. Sharf, Literature survey of contact dynamics modelling, Mech. Mach. Theory 37 (10) (2002) 1213–1239.
[19] N. Diolaiti, M. Claudio, S. Stefano, Contact impedance estimation for robotic systems, IEEE Trans. Rob. 21 (5) (2005) 925–935.
[20] K. Hunt, F. Crossley, Coefficient of restitution interpreted as damping in vibroimpact, ASME/J. Appl. Mech. 42 (June) (1975) 440–445.
[21] Barrett Technology, wiki support. http://support.barrett.com/wiki/Hand/280/
[22] L. Liu, G. Liu, Y. Zhang, Grasping control in three-fingered robot hand teleoperation using desktop haptic device[M], in: Haptics: Neuroscience, Devices, Modeling, and Applications, Springer, Berlin Heidelberg, 2014, pp. 232–240.